The International Journal of Engineering and Science (IJES)
|| Volume || 13 || Issue || 4 || Pages || PP 75-88 || 2024 ||
ISSN (e): 2319 – 1813 ISSN (p): 2319 – 1805

Load testing and structural performance evaluation of concrete box beam bridge

Yi X[1], Linshu L[1*], Yuexing W[1], Jun H[1], Xinzhong W[1], Mei W[2], Xianliang T[1]
[1] *College of Civil Engineering, Hunan City University, Yiyang, China*
[2] *Hunan Art and crafts vocational college, Yiyang, China*
Corresponding Author: Linshu L

--*ABSTRACT*--
Concrete box girder bridge has been widely used due to its advantages of high structural stiffness, smooth and comfortable traffic, good seismic performance and mature construction technology. Cracks may occur in the structure due to the long-term influence of natural environment and overloading, and affect the safe bearing capacity of the structure. Therefore, finite element method is used to analyze its vibration mode characteristics, and static load and dynamic load tests are combined to analyze its actual working state and bearing capacity. The research results indicate that the structural performance of the bridge remains good, but the actual carrying capacity has decreased due to the structural damage and cracks caused by long-term service. The findings of the study can provide reference for the maintenance and reinforcement and strengthening of similar in-service bridges.

KEYWORDS;- *Concrete box girder bridge; Finite element modeling analysis; Static load test; Dynamic load test; Structural performance evaluation*

Date of Submission: 05-04-2024 Date of acceptance: 17-04-2024

I. INTRODUCTION

In recent years, with the rapid development of the world transportation industry, bridges play an increasingly important role as transportation hubs. But the actual performance and load standard of most existing bridges can't meet the demand of existing transportation development. In order to improve the load grade and bearing capacity of the bridge and meet the purpose of bridge safety. Load tests are the most common method for evaluating existing bridges [1]. And it can judge the mechanical properties of bridges under static and dynamic loads through tests [2-11]. Zeng Yong et al. [12] conducted static load test research on actual carrying capacity and structural deformation of single-box double-cell continuous curved box girder bridge under normal service conditions. The results show that the measured curves of deflection and stress were in good agreement with the theoretical curves. Fu Quanchen [13] tests whether the carrying capacity of simply supported steel box girder bridge meets the requirements. And the stress, strain and deflection values were analyzed comparatively under load test conditions. Huang Hao et al. [14] studied a continuous box girder bridge in Fujian Province. And finite element method is used to model and analyze the bridge. The surface observation and load test of the completed bridge span structure were carried out to verify the actual state of the bridge, and the correct use and maintenance strategy was formulated. The health condition and actual load-carrying capacity of concrete girder bridges during service have always been the focus of attention of scholars all over the world [15-20].

This article conducts on-site load tests and finite element modeling analysis on a 3*20m concrete box girder bridge to study its structural performance and actual bearing capacity, providing corresponding references for similar research on structural performance and maintenance reinforcement.

II. Engineering Overview

This bridge is an existing river-crossing bridge in a certain-yang-city project. The bridge layout is a 3*20m concrete box girder bridge, with reinforced concrete box girders for all three spans and box height of 1.4m. Bridge width: 11m (Carriageway) +2*2.5m (sidewalk) +2*0.25(railing), full width 16.5m, reinforced concrete circular pier pile foundation is adopted for bridge substructure, and its concrete strength is C30. Gravity type U-shaped abutment pile foundation is adopted for abutment. The test materials：

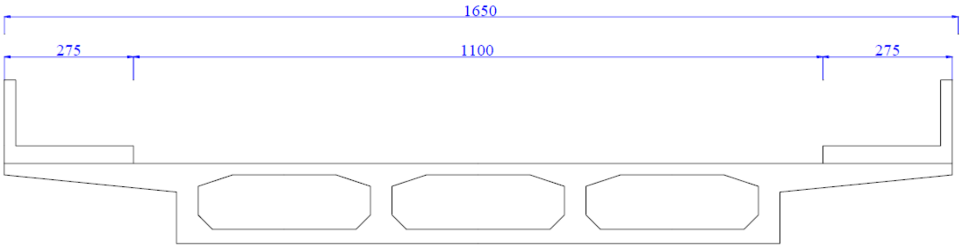

Figure 1. Schematic Diagram of Box Girder Cross Section

III. Finite element modeling analysis

According to the structural form of the bridge, the specialized program Midas Civil for bridge structural analysis was used to establish an overall structural model of the bridge for calculation and analysis. The beam element was used to simulate the main beam, the internal force and displacement of the control section were calculated, and the strain of the measuring point was solved by the theory of material mechanics. According to the as-built drawings, the load distribution position should be determined according to the relevant provisions on transverse arrangement of vehicles in "General Specification for Design of Highway Bridges and Culverts" (JTJ021 -89) [21]. The specific loading position should be consistent with the load distribution position during actual test. Please refer to the test load layout diagram. Calculate the most unfavorable internal force produced by the test load on the control section of the structure respectively, and carried out equivalent loading according to this internal force value.

The bridge calculation parameters are shown in Table 1. The finite element analysis model consisted of 305 nodes and 544 elements, Please refer to Figure 2 for details. The results of the structural live load internal force envelope diagram output by Midas Civil are shown in Figures 3~5. According to the maximum positive moment section, the maximum negative moment section and the maximum shear section of the structure, the test control section was selected. By applying load loading and working condition optimization principle, the most unfavorable internal force of calculated load on each control section of the structure is obtained respectively, and equivalent loading is carried out according to this internal force value.

Table 1 Bridge calculation parameter

Number	Parameter name	Parameter values
1	Design load grade	automobile-20、trauler-120level、crowd-3.5kN/m2
2	Concrete strength grade	C30
3	Calculated span (m)	3*20
4	Clear width of bridge deck (m) and number of lanes	16.5m、three-lane
5	Straight Bridge/Curved Bridge (Radius)	straight line segment

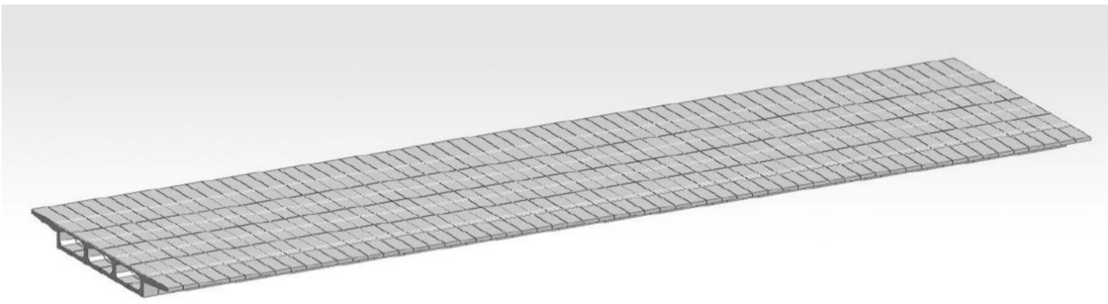

Figure 2 Bridge structure finite element calculation node model diagram

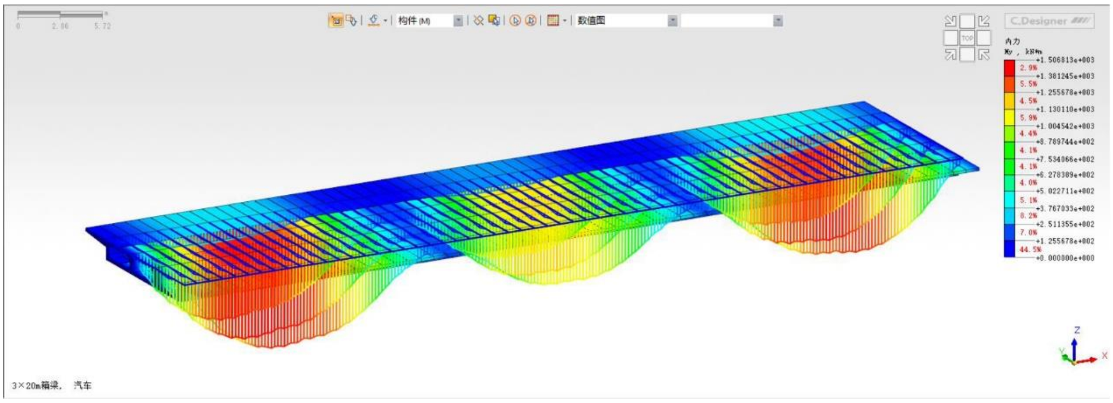

Figure 3 Envelope Diagram of Moment under Moving Load

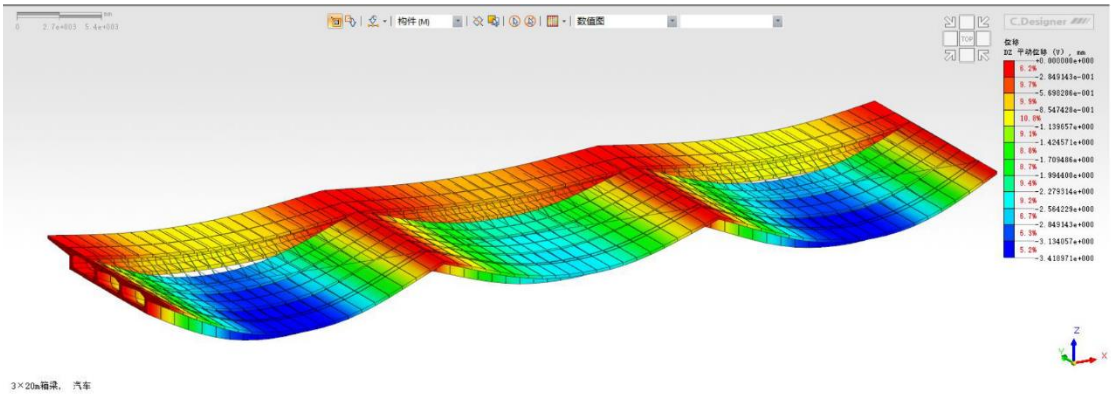

Figure 4 Displacement variation diagram under moving load

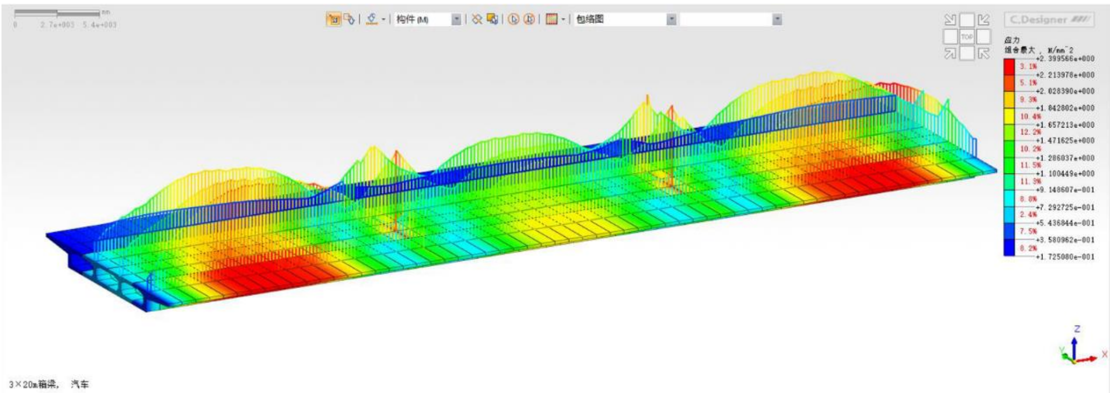

Figure 5 Stress envelope diagram under moving load

IV. Static Load Test Study and Structural Performance Evaluation

Test point layout and test conditions

According to the bridge structure model, the mechanical characteristics of the bridge and JTG/T J21-2011 " Code for testing and evaluating bearing capacity of highway bridges "[22] and combined with the settlement results, the bridge will be arranged according to the following conditions and test conditions.

Test point layout:

1）Layout of strain test points

To analyze the strain magnitude of the test span under the test load, three strain test points were arranged at the mid span section of the three spans in this experiment, respectively, on the bottom plate of the box girder, as shown in Figure 6. Arrange temperature compensation patches at the position of each test section to counteract the impact of temperature changes on the test strain (stress).

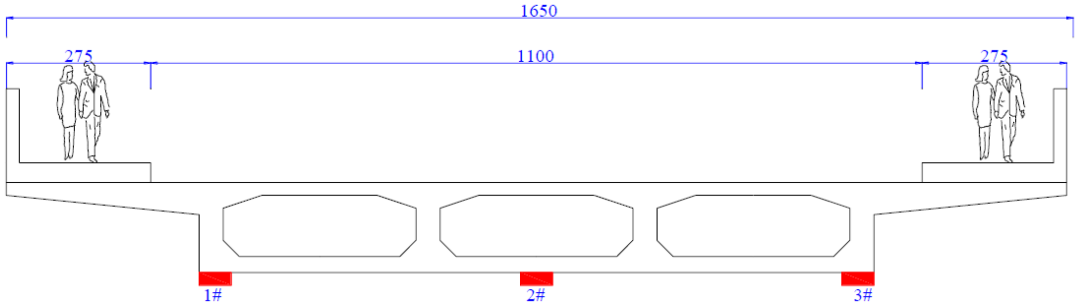

Figure 6 Schematic diagram of strain test point arrangement

2）Deflection testing

The longitudinal bridge was arranged according to the four equally divided points of the span

The transverse bridge direction was arranged the centerline position of each beam, as shown in Figure 7.

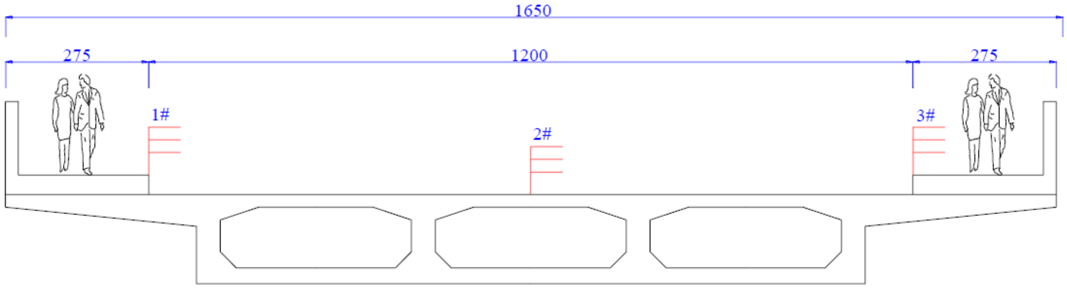

Figure 7 Horizontal layout diagram of bridge deck deflection measurement points

Test conditions:

Based on the stress characteristics of the bridge and calculation results, the main test sections and test conditions of the test are as follows:

1）Maximum positive moment condition of the first span, hereinafter called ①

2）Maximum negative moment condition of 1#，hereinafter called ②

3）Maximum positive moment condition of the second span hereinafter called ③

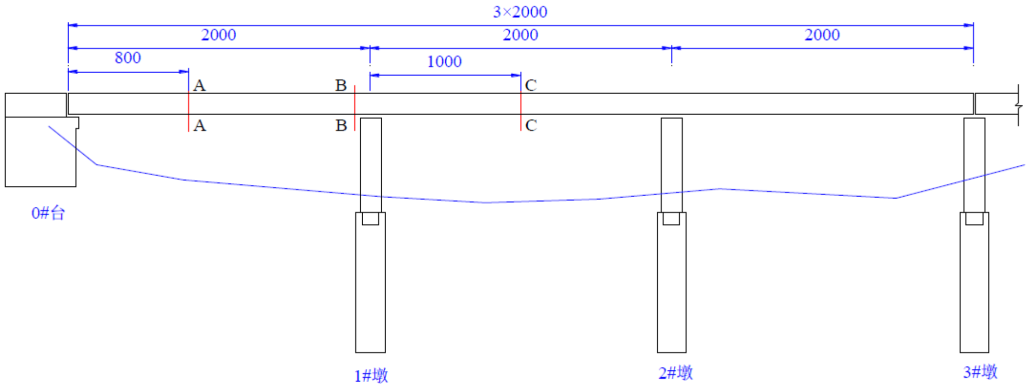

Figure 8 Location diagram of test section under test condition（cm）

Table 2 Condition Setting Statistics

Condition number	Condition name	Control section	Test content
Condition I	①	A-A	Deflection, strain, cracks
Condition II	②	B-B	Strain, cracks
Condition III	③	C-C	Deflection, strain, cracks

Layout of experimental loading conditions

According to the control section of the internal force influence line, using 380kN loading vehicle for equivalent loading, made the control section internal force to achieve the maximum under the action of design live load. Loading was divided into three levels, from zero to the maximum value step by step, and unloading was performed at the first level.

The positions of loading vehicles under working conditions I - III were shown in Figure 9-11 respectively.

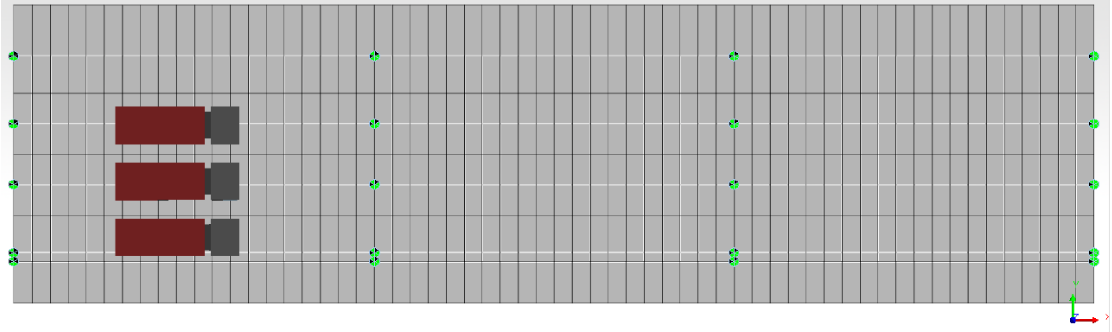

（a）

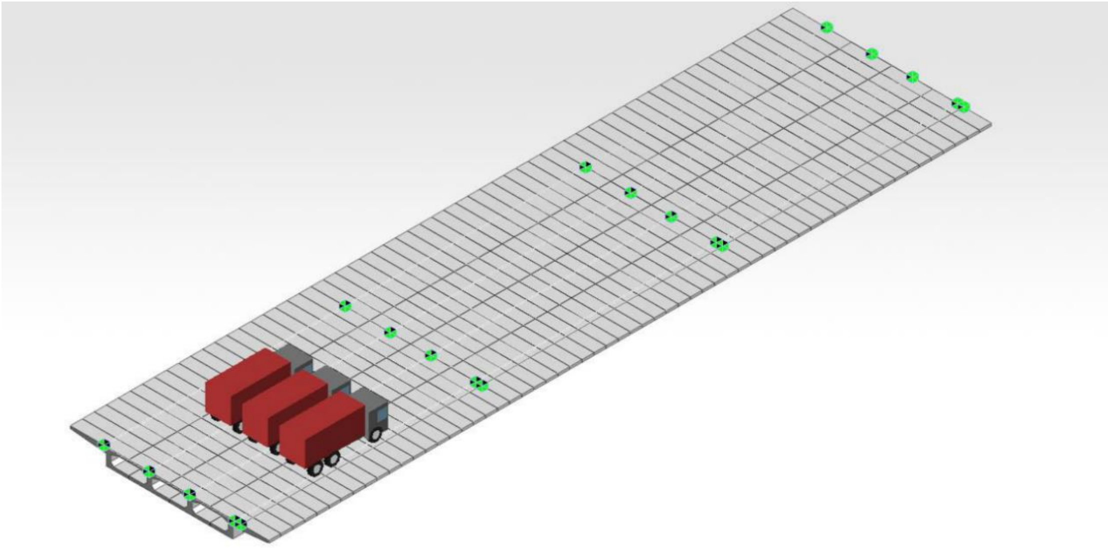

（b）

Figure 9 Condition I schematic diagram of loading vehicle position

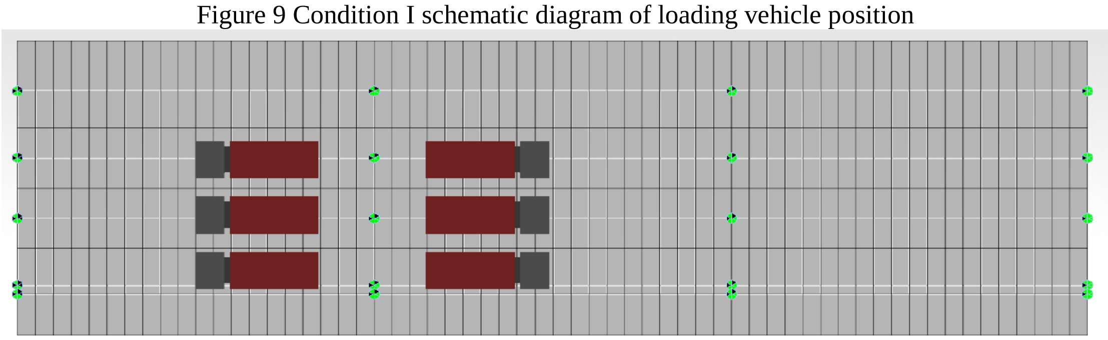

（a）

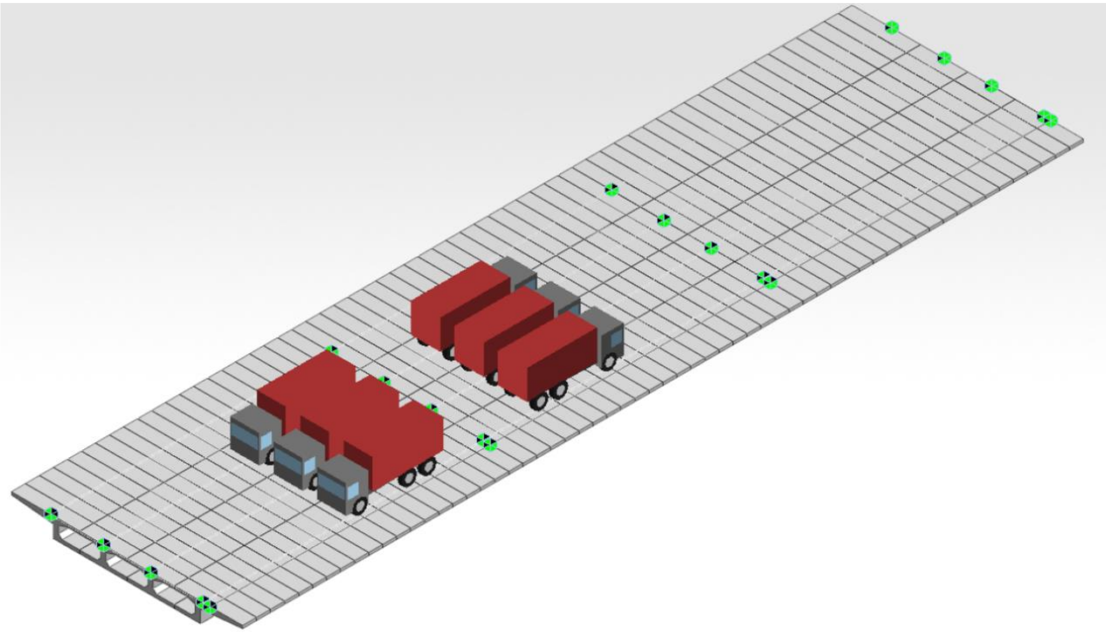

（b）

Figure 10 Condition II schematic diagram of loading vehicle position

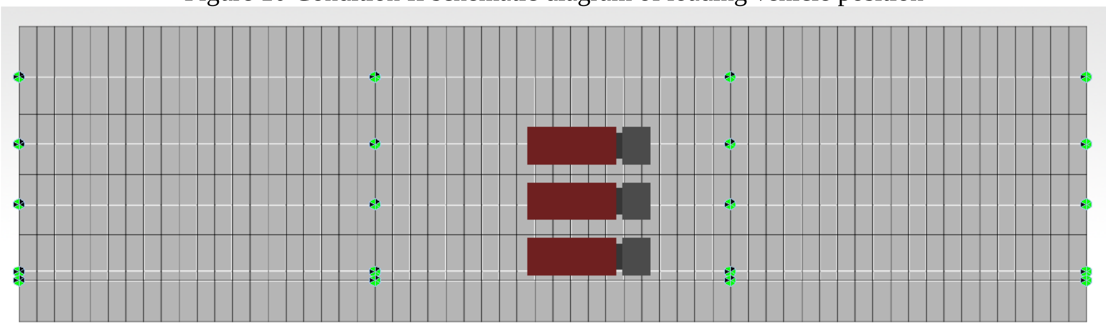

（a）

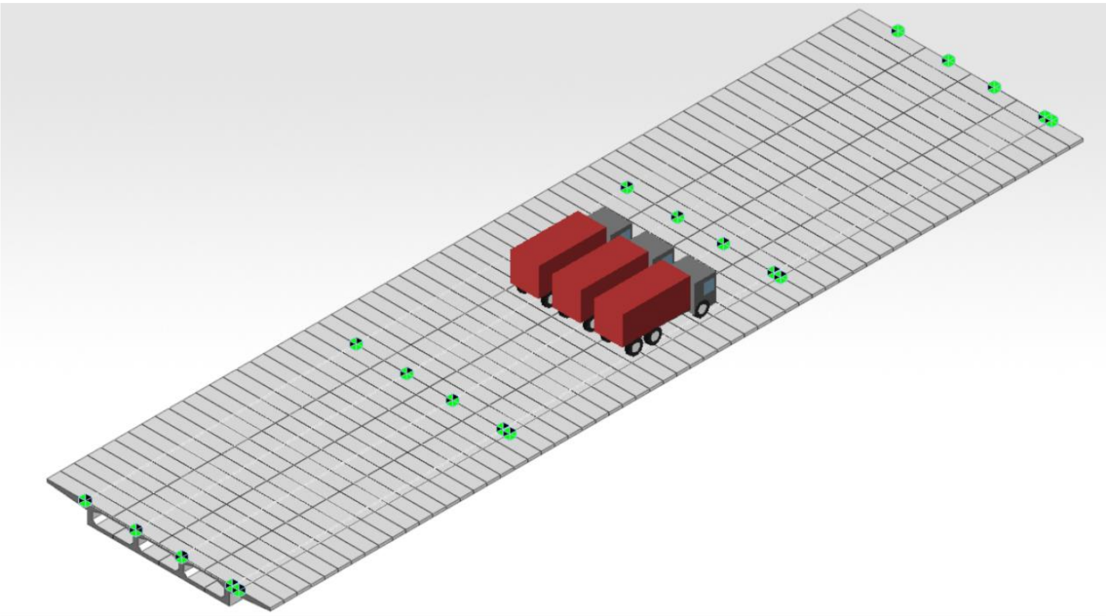

（b）

Figure 11 Condition III schematic diagram of loading vehicle position

Static Load Result Analysis and Performance Evaluation

Static load results:

The linear variation of strain and deflection of three sections under partial load, the longitudinal distribution of deflection under full load, the deviation between measured value and calculated value, and the elastic recovery after unloading can be mastered by graded loading. The test results are shown in the table below.

Table 3 Load test loading efficiency

Load condition	Controller （kN*m）	Target value （kN*m）	Loading efficiency	Maximum load efficiency	Minimum load efficiency
①	1503（39I）	1428	0.95	1.05	0.95
②	-1068（50I）	-1032	0.97	1.05	0.95
③	1203（118I）	1179	0.98	1.05	0.95

Table 4 Deflection test results of measuring points of each section under various loading condition

Condition	Section	Point number	Project	nitial value	The first stage	The second stage	The third stage	Unloadin g value
Condition I	A-A	1#point	Calculated value（με）	0.00	-1.57	-2.88	-3.35	0.00
			Actual measured value（με）	0.00	-1.15	-2.05	-2.63	-0.18
		2#point	Calculated value（με）	0.00	-1.42	-2.61	-3.03	0.00
			Actual measured value（με）	0.00	-1.07	-1.86	-2.28	-0.16
		3#point	Calculated value（με）	0.00	-0.40	-0.73	-0.85	0.00
			Actual measured value（με）	0.00	-0.26	-0.48	-0.61	-0.06
Condition III	C-C	1#point	Calculated value（με）	0.00	-1.22	-2.26	-2.54	0.00
			Actual measured value（με）	0.00	-0.88	-1.58	-1.97	-0.14
		2#point	Calculated value（με）	0.00	-1.16	-2.15	-2.42	0.00
			Actual measured value（με）	0.00	-0.81	-1.36	-1.81	-0.16
		3#point	Calculated value（με）	0.00	-1.08	-2.01	-2.26	0.00
			Actual measured value（με）	0.00	-0.74	-1.24	-1.61	-0.12

Table 5 Strain test results of measuring points of each section under various loading conditions

Condition	Section	Point number	Project	Initial value	The first stage	The second stage	The third stage	Unloadin g value
Condition I	A-A	1#point	Calculated value（με）	0	34	60	70	0
			Actual measured	0	24	39	51	3

			value（με）					
		2#point	Calculated value（με）	0	29	52	61	0
			Actual measured value（με）	0	21	29	42	2
		3#point	Calculated value（με）	0	27	48	56	0
			Actual measured value（με）	0	18	29	37	2
Condition II	B-B	1#point	Calculated value（με）	0	-22	-42	-49	0
			Actual measured value（με）	0	-15	-27	-35	-2
		2#point	Calculated value（με）	0	-20	-39	-46	0
			Actual measured value（με）	0	-14	-23	-31	-2
		3#point	Calculated value（με）	0	-18	-34	-40	0
			Actual measured value（με）	0	-11	-18	-25	-1
Condition III	C-C	1#point	Calculated value（με）	0	22	41	46	0
			Actual measured value（με）	0	17	26	35	3
		2#point	Calculated value（με）	0	21	38	43	0
			Actual measured value（με）	0	14	22	31	2
		3#point	Calculated value（με）	0	19	36	40	0
			Actual measured value（με）	0	13	21	28	2

The following conclusions can be drawn from the above graphs:

1）The measured strain at the bottom of the three beams keeps linear increase during loading, and the measured strain at No. 1 ~ No. 3 measuring points is less than the calculated value, and basically recovers after unloading.

2）The measured strain distribution of three sections under full load is basically consistent with the calculated strain distribution, and the measured strain distribution is smaller than the calculated strain distribution.

Evaluation of Static Load Test Results：

The test results are evaluated according to the Code for Testing and Evaluation of Bearing Capacity of Highway Bridges (JTG/T J21-2011)[22].

Testing coefficient η：

Calibration coefficient refers to the ratio of measured elastic value and corresponding calculated value of a certain measuring point. Under the same load, the measured elastic value should be close to the calculated value; when $\eta<1.00$, it indicates that the working performance of the structure is better and meets the requirements of use.

$$\eta = \frac{S_e}{S_s}$$

Formula： S_e ——Test elastic displacement or strain value of main measuring point under test load；

S_s ——Theoretical calculated displacement or strain values of main measuring points under test load.

The stress and deflection calibration coefficients and evaluation of the main measurement points for this experiment are shown in Table 5 below.

Table 6 Evaluation Table for Verification Factors of Various Operating Conditions

Condition	Project	Number	Calculated value	Elastic value	Testing coefficient	Result
Condition I	Deflection（mm）	H1	-3.35	-2.45	0.73	Satisfy
		H2	-3.03	-2.12	0.70	Satisfy
		H3	-0.85	-0.55	0.65	Satisfy
	Strain（με）	1#	70	48	0.68	Satisfy
		2#	61	40	0.65	Satisfy
		3#	56	35	0.62	Satisfy
Condition II	Strain（με）	1#	-49	-33	0.67	Satisfy
		2#	-46	-29	0.64	Satisfy
		3#	-40	-24	0.61	Satisfy
Condition III	Deflection（mm）	H1	-2.54	-1.83	0.72	Satisfy
		H2	-2.42	-1.65	0.68	Satisfy
		H3	-2.26	-1.49	0.66	Satisfy
	Strain（με）	1#	46	32	0.70	Satisfy
		2#	43	29	0.68	Satisfy
		3#	40	26	0.64	Satisfy

From the above table, it can be seen that the strain verification coefficient is between 0.62 and 0.70, and the deflection verification coefficient is between 0.65 and 0.73. The strain verification coefficients are all less than 1.0, and the deflection verification coefficients are all less than 1.00, meeting the requirements of the specifications.

Residual deformation assessment

Relative residual displacement or relative residual strain ΔS_p is the ratio of the measured residual displacement or strain at a measuring point to the corresponding measured total displacement or strain。The smaller ΔS_p indicates that the structure is closer to elastic working condition。When the relative residual displacement or relative residual strain of the main measuring points exceeds 20%, it should be judged that the bearing capacity of the bridge does not meet the requirements.

$$\Delta S_p = \frac{S_p}{S_t} \times 100\%$$

Formula: S_p ——The measured residual displacement or residual strain of the main measuring points;

S_t ——The measured total displacement or total strain of the main measuring points under experimental load.

The main measurement points for stress, residual deflection values, and evaluation in this experiment are shown in Table 7 below.

Table 7 Residual deformation evaluation table under various working conditions

Condition	Project	Point number	Calculated value	Elastic value	Residual deformation（%）	Result
Condition I	Deflection（mm）	H1	-2.63	-0.18	6.86	Satisfy
		H2	-2.28	-0.16	7.01	Satisfy
		H3	-0.61	-0.06	9.80	Satisfy
	Strain（με）	1#	51	3	5.93	Satisfy
		2#	42	2	4.80	Satisfy
		3#	37	2	5.45	Satisfy

Condition II	Strain（με）	1#	-35	-2	5.74	Satisfy
		2#	-31	-2	6.36	Satisfy
		3#	-25	-1	3.94	Satisfy
Condition III	Deflection（mm）	H1	-1.97	-0.14	7.11	Satisfy
		H2	-1.81	-0.16	8.86	Satisfy
		H3	-1.61	-0.12	7.45	Satisfy
	Strain（με）	1#	35	3	8.52	Satisfy
		2#	31	2	6.40	Satisfy
		3#	28	2	7.25	Satisfy

It can be seen from the above table that the relative residual deformation of each strain measuring point is between 3.94% and 8.52%, which is less than 20%, meeting the specification requirements; the relative residual deformation of each deflection measuring point is between 6.86~9.80%, which is less than 20%, meeting the specification requirements.

3）Evaluation of structural strength and stiffness

According to Code for Testing and Evaluating Bearing Capacity of Highway Bridges (JTG/TJ21 - 2011)[22], it shall be judged that the bearing capacity of bridges does not meet the requirements when one of the following conditions occurs：

（1）Static load test calibration coefficient of main measuring points is greater than 1.00.

（2）Relative residual deformation or relative residual strain of main measuring points exceeds 20%.

（3）The crack propagation width under test load exceeds the specification limit, and the crack closure width after unloading is less than 2/3 of the propagation width.

（4）Under the test load, the bridge foundation has unstable settlement displacement.

According to the test results, the static load test calibration coefficients of the main control points of the 3× 20m continuous box girder are all less than 1.00, the relative residual deformation or relative residual strain of the main measuring points are all less than 20%, no cracks are found in the test process, and no unstable settlement displacement occurs in the bridge foundation. Therefore, it can be judged that the bearing capacity of the bridge meets the requirements.

V. Dynamic Load Test Research and Structural Performance Evaluation

Under dynamic loads such as moving vehicles, people, wind and earthquake, bridges will produce dynamic responses such as vibration and impact, which are not only related to the structural characteristics (mass, stiffness and damping) of bridges and vehicles, but also to the interaction of two vibration systems of bridges and loads, the speed of vehicles and the flatness of bridge decks. The dynamic characteristics of bridge structure are important parameters for evaluating the bearing capacity of bridge, and also important parameters for identifying the working performance of bridge structure and seismic analysis of bridge [22].

Measurement point arrangement and loading condition of dynamic load test

(1) Fluctuation test

1)Test item content

The main items of pulsation test are natural frequency, vibration mode and damping ratio of bridge span structure.

2)Test section and test point arrangement The test section of pulsation test is arranged at the mid-span mid-section.

(2) Sports car test

1) The test items mainly test the time-history stress curve of the bridge span structure under dynamic load, and obtain the maximum dynamic strain and impact coefficient of the bridge span structure through analysis.

2) Test section and test point layout

The test section of road test shall be arranged at the maximum positive moment section of corresponding bridge span.

Test method (1) Vibration acceleration of measuring points: The random vibration response of the bridge structure is picked up and recorded through vibration sensors, amplifiers, signal acquisition systems, and computers;（2）Measurement of point dynamic strain: Resistance strain gauges are used for testing.

Analysis of Dynamic Load Test Results and Performance Analysis

Analysis of dynamic characteristics of bridge span structures

The measured vertical first-order frequencies are all greater than the calculated frequencies, indicating that the vertical dynamic stiffness index of the structure is good, and the measured damping ratio is within the normal range. The detailed test results are shown in Table 7, and the measured fundamental frequency is shown in Figures 12 and 13.

Table 8 Test results of structural natural vibration characteristic parameters

number	fundamental frequency	Actual measured frequency （Hz）	Calculate frequency （Hz）	Measured damping ratio （%）	Actual measured frequency/calculated frequency
1	First derivative	7.61	6.71	1.196	1.13

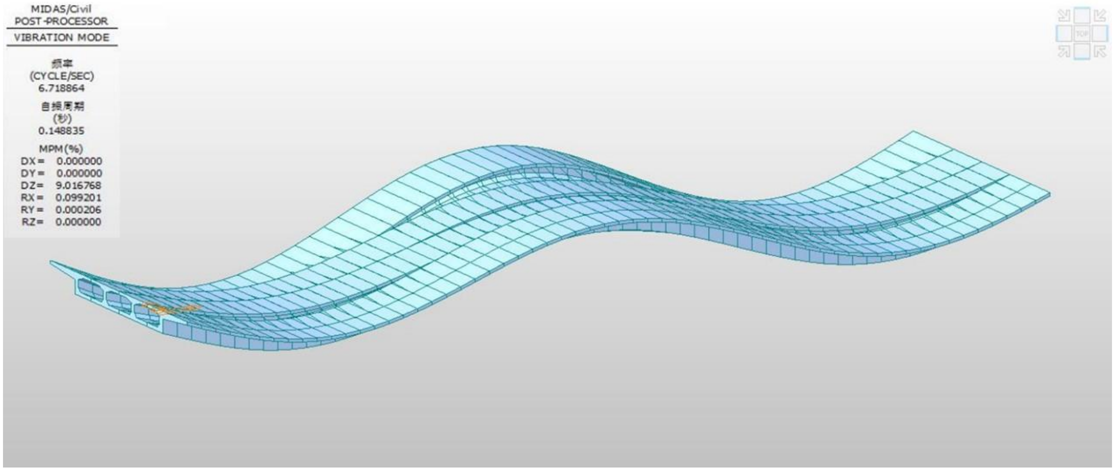

Figure 12 Theoretical first-order fundamental frequency

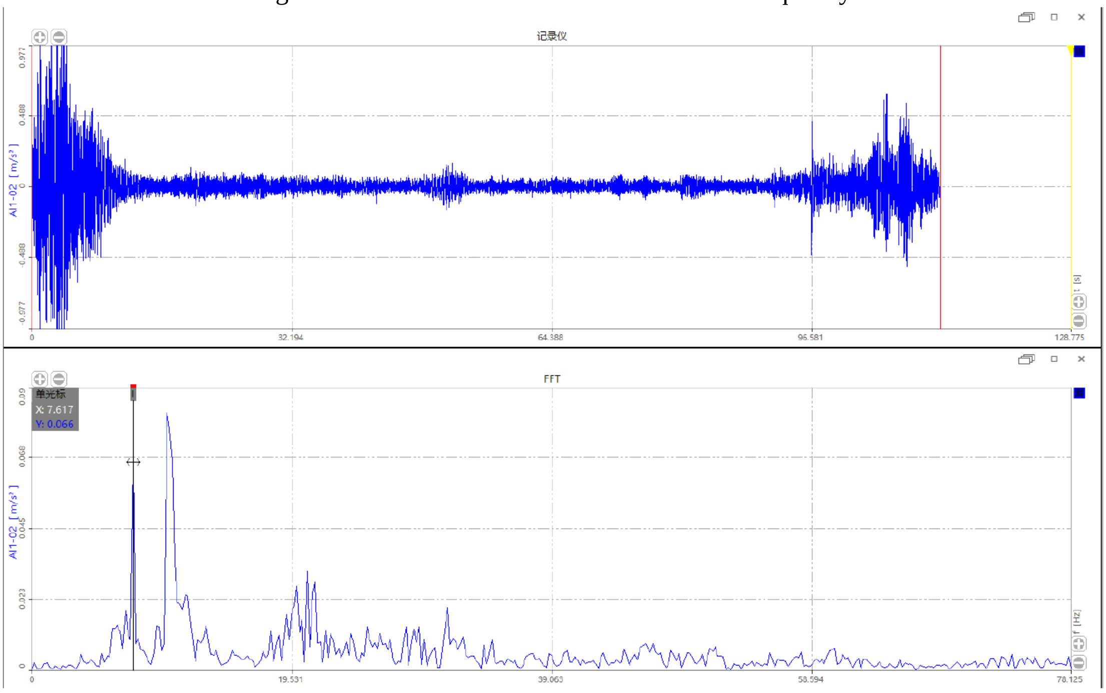

Figure 13 Tested first-order fundamental frequency

Dynamic response analysis of driving test

The sports car operating conditions are based on a speed of 10km/h for one working condition, and braking at 5km/h and 10km/h for a total of two working conditions. The dynamic response detection results of the sports car and brake test structures are shown in Table 9.

Table 9 Driving test power response detection results

sectional position	point	Condition		
		10Km/h Sports car	5km/h brake	10km/h brake
Mid-section of the first span	1#	48	42	40
	2#	47	46	42
Mid-section of the second span	1#	1.18	1.16	1.15
	2#	1.18	1.16	1.15

The typical test signal for working conditions is shown in Figure 14.

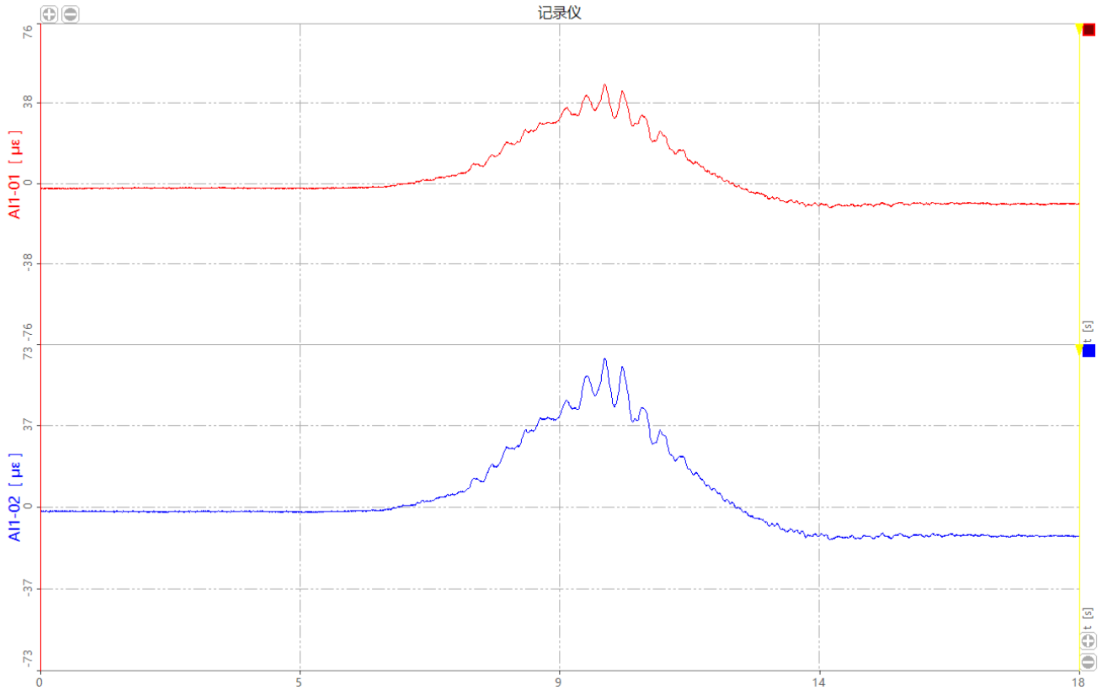

（a）10km/h Dynamic response of sports car test section

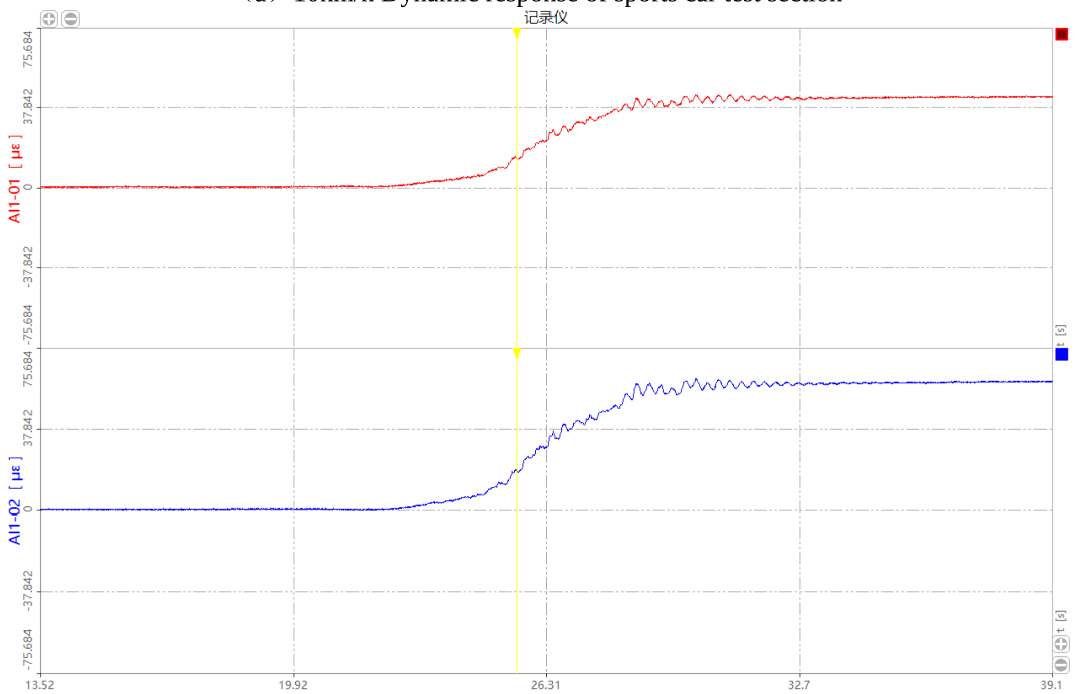

（b）5km/h Dynamic response of brake test section

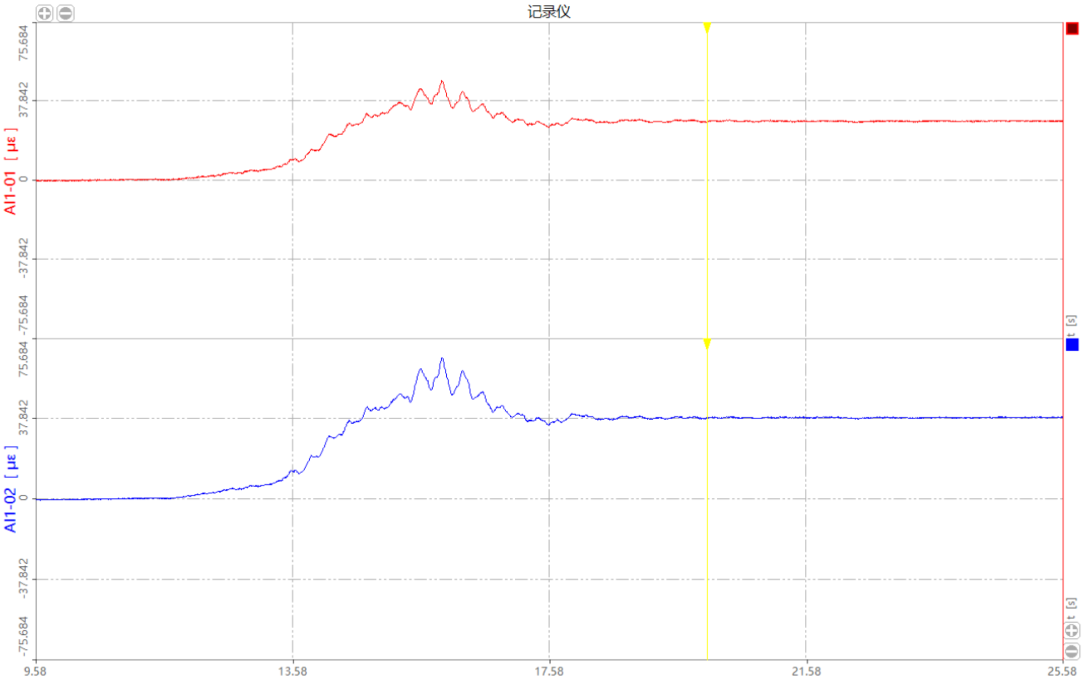

（c）10km/h Dynamic response of brake test section

Figure 14 Typical working condition test signal diagram

VI. CONCLUSION

Through static and dynamic load test and numerical simulation of concrete box girder bridge in a certain Yangshi project, the selection of test control section and loading condition is guided by the finite element analysis results, and then the strain and deformation of each main control section are tested and analyzed through the test.

1) Static load test condition loading efficiency is 0.95~1.00, meet the specification requirements.

2) In the process of graded loading under each working condition, the measured strain and deflection values of main control measuring points of control section keep linear growth, and the linear relationship is good, and both are less than the calculated values; under full load, the longitudinal deflection of test cross-measuring points is good, the measured distribution law is consistent with the calculated values, and the measured values are less than the calculated values.

3) The relative residual deformation or relative residual strain of main control measuring points of control section under each working condition is less than 20. The test span beam body is in elastic working state; the calibration coefficients of main deflection measuring points of control section under each working condition are less than 1.00, and the calibration coefficients of strain measuring points are less than 1.00. The structural strength and stiffness of the bridge meet the specification requirements.

4) The first order natural frequency of the bridge is obtained through calculation and analysis, the measured vertical first order frequency is greater than the calculated frequency, the measured damping ratio is within the normal range, and the dynamic characteristics are normal; the measured impact coefficient is less than the theoretical calculation value, indicating that the bridge structure has good driving performance.

To sum up, the bearing capacity and structural stiffness of the main control sections of the bridge meet the design requirements, and the basic dynamic characteristics of the test span structure are good. Considering the safety of the bridge structure, when evaluating the performance of the same kind of bridge structure, we should pay attention to the damaged parts of the bridge structure, such as cracks, and strengthen and repair them accordingly.

FUNDING

The author(s) declare that financial support was received for the research, authorship, and/or publication of this article. This research was funded by National Undergraduate Innovation and Entrepreneurship Plan Program, China (202211527028), Undergraduate Innovation and Entrepreneurship Training Plan Program of Hunan Province, China (S202311527025).

REFERENCE

[1]. Shuanhai H, Xiangmo Z, Jian M, et al. Review of Highway Bridge Inspection and Condition Assessment. [J]. China Journal of Highway and Transport, 2017,30(11):63-80.
[2]. Zhouhong Z, Weixin R, Zhengfei Z, et al. Load-carrying capacity assessment methods of existing bridges. [J]. Earthquake Engineering and Engineering Dynamics, 2005(05):149-154
[3]. Miaoyi D, Weixin R. Continuous box-girder bridge structure finite element model updating based on static-load testing.[J]. Journal of Fuzhou University(Natural Science Edition), 2009,37(02):261-266.
[4]. Xingjun Q, Sheng Q, Xufa S, et al. Rapid stiffness evaluation of prefabricated simply supported beam bridge based on modal test and equivalent load. [J]. Journal of Architecture and Civil Engineering, 2023,40(04):117-124.
[5]. Yulun W, Zejun Z, Liangdong Z, et al. Load Test of Bridge with Multiple Steel Box Girders and Composite Deck Slabs After Completion and Parametric Analysis. [J], Bridge Construction, 2023,53(05):90-96.
[6]. Bayraktar, Alemdar, Temel Türker, Janusz Tadla, Altok Kurşun, and Arif Erdiş. Static and dynamic field load testing of the long span Nissibi cable-stayed bridge [J]. Soil Dynamics and Earthquake Engineering 94 (2017): 136-157.
[7]. Cao, Wen-Jun, Chan Ghee Koh, and Ian FC Smith. Enhancing static-load-test identification of bridges using dynamic data. [J] Engineering Structures 186 (2019): 410-420.
[8]. De Angelis, Alessandra, and Maria Rosaria Pecce. Model assessment of a bridge by load and dynamic tests. [J] Engineering Structures 275 (2023): 115282.
[9]. Lu, Pengzhen, Zijie Xu, Yangrui Chen, and Yutao Zhou. Prediction method of bridge static load test results based on Kriging model [J]. Engineering Structures 214 (2020): 110641.
[10]. Guan, Ze-Xin, Dong-Hui Yang, Ting-Hua Yi, Wen-Jie Li, and Chong Li. Bridge finite element model updating using stochastic vehicle-induced static response monitoring data [J]. Engineering Structures 301 (2024): 117280.
[11]. Wang, Ning-Bo, Wei Shen, Chuanrui Guo, and Hua-Wan. Moving load test-based rapid bridge capacity evaluation through actual influence line [J]. Engineering Structures 252 (2022): 113630.
[12]. Yong Z, Xudong S, Guanglie C, et al. Static load test of single box double chamber continuous curved box girder bridge. [J], Journal of Luoyang Institute of Science and Technology(Natural Science Edition), 2021,31(03):30-38.
[13]. Quancheng F. Simply supported steel mixed box girder load test analysis and research. [J]. Communications Science and Technology Heilongjiang, 2023,46(08):80-82.
[14]. Hao H, Yixiong Z, Tangyan D. Bearing capacity assessment of continuous box girder bridge based on static dynamic load test. [J], China Construction, 2024(01):163-165.
[15]. Tong, Kai, Hong Zhang, Ruiqiang Zhao, Jianting Zhou, and Huajian Ying. Investigation of SMFL monitoring technique for evaluating the load-bearing capacity of RC bridges [J]. Engineering Structures 293 (2023): 116667.
[16]. Gao, Xu, Yuqing Liu, Yangqing Liu, and Dalei Wang. Experimental and analytical study on compressive bearing capacity of steel shell-concrete composite bridge tower [J]. Engineering Structures 278 (2023): 115567.
[17]. Šomodíková, Martina, David Lehký, Jiří Doležel, and Drahomír Novák. Modeling of degradation processes in concrete: Probabilistic lifetime and load-bearing capacity assessment of existing reinforced concrete bridges [J]. Engineering Structures 119 (2016): 49-60.
[18]. Bautista-De Castro, Álvaro, Luis Javier Sánchez-Aparicio, Luís F. Ramos, José Sena-Cruz, and Diego González-Aguilera. Integrating geomatic approaches, Operational Modal Analysis, advanced numerical and updating methods to evaluate the current safety conditions of the historical Bôco Bridge [J]. Construction and Building Materials 158 (2018): 961-984.
[19]. Yuefei, Liu, Lu Dagang, and Fan Xue. Reliability updating and prediction of bridge structures based on proof loads and monitored data [J]. Construction and Building Materials 66 (2014): 795-804.
[20]. JTJ 021-1989, General Specification for Highway Bridge Design [S].
[21]. JTG/T J21-2011, Specification for Bearing Capacity Testing and Evaluation of Highway Bridges [S].